

Analysis of temporal variations of surface albedo from MODIS¹

Wei Gao^{*a,e}, Qifeng Lu^{**b}, Zhiqiang Gao^{a,c,e}, Wanli Wu^d, Bingyu Du^f, and James Slusser^a

^aUSDA UV-B Monitoring and Research Program, Natural Resource Ecology Laboratory, Colorado State University, Fort Collins, CO;

^bKey Laboratory of Radiometric Calibration and Validation for Environmental Satellites, China Meteorological Administration (LRCVES/CMA), Beijing, China;

^cInstitute of Geographic Sciences and Natural Resources Research, The Chinese Academy of Sciences, Beijing, China;

^dClimate and Global Dynamics Division, National Center for Atmospheric Research, Boulder, CO;

^eInternational Center for Desert Affairs-Research for Sustainable Development in Arid and Semi-Arid Lands, Urumqi, China;

^fNanjing University of Information Science & Technology, Nanjing, China

ABSTRACT

Land surface albedo is a key parameter in modeling radiative transfer in the atmosphere. Simulated climates are sensitive to specified albedo in models. The MODIS BRDF/Albedo Science Data Product represents the latest attempt at providing a dataset suitable for climate model comparisons. It is necessary to analyze the feature of white-sky and black-sky albedo before its use in land surface models. White-sky (diffuse) and black-sky albedo (direct at local solar noon) in China from MODIS based on Lucht algorithm are calculated and analyzed. The differences of white-sky and black-sky albedo for different land use/land cover are compared. The derived albedo exhibits clear interannual variation with large variation in Northern China. Black-sky albedo and white-sky albedo are characterized with different features for different land covers.

Key words: Temporal variations, Albedo, MODIS, Black sky, White sky

1.INTRODUCTION

Surface albedo, the ratio of upwelling irradiance to the down-welling irradiance incident upon a surface, determines in large part the amount of energy available to drive turbulent fluxes of heat and moisture. Land surface albedo is a key parameter in modeling radiative transfer in the atmosphere, and climate models are sensitive to the specification of land surface albedo^[1-6]. Albedo is one crucial path to understanding feedback mechanisms between radiation balance and its influence on climate and vegetation dynamics^[7-11], and also one important source contributing to uncertainties in radiative computation. A high accurate albedo is required for a quality climate simulation^{[7],[12]}. Satellite remote sensing provides feasible technique to obtain reliable and accurate estimates of surface albedo at the global scale and with high temporal resolution^[13-15]. The MODIS BRDF/Albedo Science Data Product represents the latest attempt at providing a dataset that is suitable for climate model comparisons^[16].

Albedo is a standard product derived from the data acquired by the Moderate Resolution Imaging Spectroradiometer (MODIS) on the Earth Observing System (EOS) AM-1 platform^[17] launched on Dec. 18, 1999. Using seven spectral channels between 470-nm and 2,130-nm wavelengths, this product provides spectral and broadband albedo once every 16 days in the visible, near-infrared, and total shortwave bands.

The objectives of this paper are 1) to examine seasonal and interannual variability in derived black-sky and white-sky albedo with emphases on the application of such product for land surface model, and 2) to analysis dependence of black-sky and white-sky albedo on land covers.

¹ Address correspondence to: * wgao@uvb.nrel.colostate.edu, phone (970) 491-3609, fax (970) 491-3601;

** lqifeng@163.com, phone 86-10-64889847

2. ALGORITHM DESCRIPTION

The operationally archived MODIS albedo products (MOD43) ^[16] include the best-fit bidirectional reflectance distribution function (BRDF) model parameters associated with the first seven spectral bands of MODIS and three additional broad-bands (0.3–0.7, 0.7–5.0, and 0.3–5.0 μm). The BRDF specifies the angular distribution of surface scattering as functions of illumination and viewing geometries at a particular wavelength. The down-welling radiative flux at the surface may be written as the sum of a direct component and a diffuse component. The directional hemispherical reflectance (black-sky albedo) is defined as the albedo in the absence of a diffuse component and is a function of solar zenith angle. The bi-hemispherical reflectance (white-sky albedo) is defined as the albedo in the absence of a direct component when the diffuse component is isotropic. The completely diffuse bi-hemispherical albedo for isotropic illumination can be derived through integration of the BRDF for the entire solar and viewing hemisphere, while the direct beam directional hemispherical albedo can be calculated through integration of the BRDF for particular illumination geometry ^[18]. Actual albedo under given atmospheric and illumination conditions can be estimated as a combination of black-sky and white-sky albedo, based on proportions of direct beam and diffuse illumination.

In addition to the BRDF model parameters, white-sky and black-sky albedo are computed for local solar noon and provided as a standard product for the same seven MODIS channel spectral bands and the three broadband regions.

The MOD43B1 BRDF/Albedo Model Parameters Product (MODIS/Terra BRDF/Albedo Model_1 16-Day L3 Global 1km SIN Grid) supplies the weighting parameters associated with the RossThickLiSparseReciprocal BRDF model that best describes the anisotropy of each pixel. These three parameters (f_{iso} , f_{vol} , f_{geo}) are provided for each of the MODIS spectral bands as well as for three broad bands (0.3-0.7 μm , 0.7-5.0 μm , and 0.3-5.0 μm). These parameters can be used in a forward version of the model to reconstruct the surface anisotropic effects and thus correct directional reflectance to a common view geometry (this is the procedure that is used to produce MOD43B4 Nadir BRDF-Adjusted Reflectance - NBAR) or to compute the integrated black-sky (at some solar zenith angle) and white-sky albedo (as is done for MOD43B3). Alternately, the parameters can be used with a simple polynomial to easily estimate the black-sky albedo with good accuracy for any desired solar zenith angle. The polynomial is as follows with constant values in the table below:

$$\alpha_{bs}(\Theta, \lambda) = f_{iso}(\lambda)(g_{0iso} + g_{1iso}\Theta^2 + g_{2iso}\Theta^3) + f_{vol}(\lambda)(g_{0vol} + g_{1vol}\Theta^2 + g_{2vol}\Theta^3) + f_{geo}(\lambda)(g_{0geo} + g_{1geo}\Theta^2 + g_{2geo}\Theta^3) \quad (1)$$

Term	Isotropic (iso)	RossThick (vol)	LiSparseR (geo)
g_0	1.0	-0.007574	-1.284909
g_1	0.0	-0.070987	-0.166314
g_2	0.0	0.307588	0.041840

Similarly, the white-sky albedo can be computed by the equation:

$$\alpha_{ws}(\lambda) = f_{iso}(\lambda)g_{iso} + f_{vol}(\lambda)g_{vol} + f_{geo}(\lambda)g_{geo} \quad (2)$$

The estimates of the white-sky kernel integrals are:

Term	Isotropic (iso)	RossThick (vol)	LiSparseR (geo)
White-sky integral g	1.0	0.189184	-1.377622

In addition to the model parameters, the MOD43B1 BRDF/Albedo Model Parameters Product also provides extensive quality information. ^[16-17, 19-20] This algorithm has been proved to be efficient ^[21-23].

3. ANALYSIS AND RESULTS

From the algorithm described above, black-sky and white-sky albedo in China from 2000 and 2001 are calculated. The albedo differences between white-sky and black-sky in various areas of China are analyzed for summer and winter seasons in 2000 and 2001.

3.1 Albedo variance at different time scales

3.1.1 Albedo differences between black-sky and white-sky albedo

Figure 1 indicates that differences are small in most areas of western China, and large differences in Tianshan Mountain, along Inner Mongolia, in the south-east area of the Tibet Plateau and in the southern area of south-western China.

The algorithm of black-sky albedo introduces the solar zenith angle relative to the one of white-sky albedo. The solar zenith angle contributes to these large differences between black-sky and white-sky. The complicated topography in combination with solar zenith angle contributes the complexity of spatial and temporal distributions of albedo.

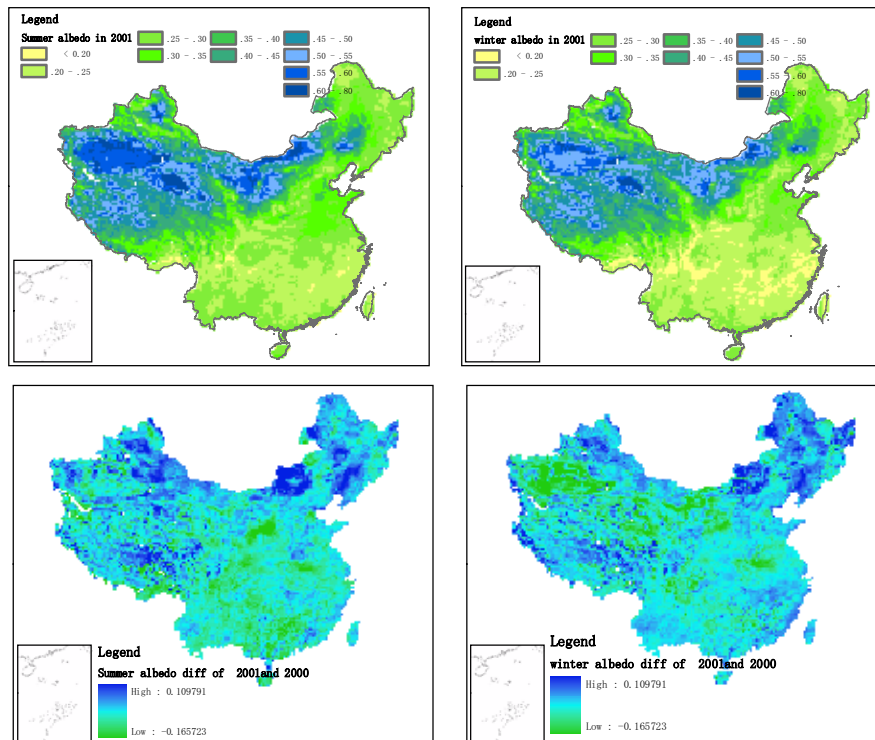


Figure 1 difference chart between black-sky and white-sky in winter and summer

3.1.2 Albedo different between 2001 and 2000

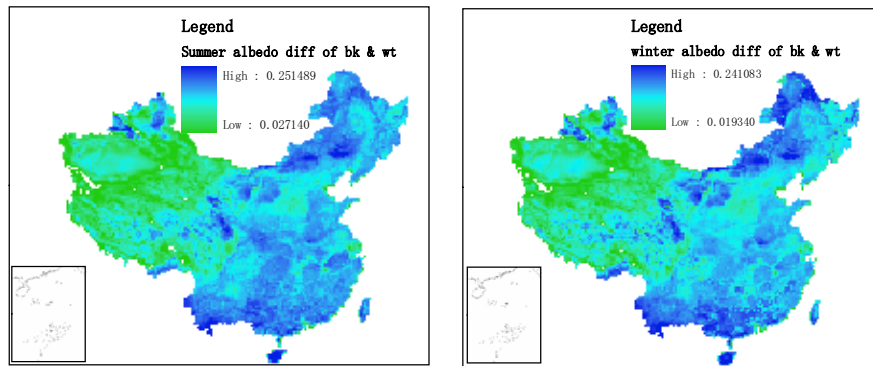


Figure 2 albedo difference chart between 2001 and 2000, bk stands for black-sky albedo and wt for white-sky albedo

Figure 2 indicates that there are large differences in most areas of east China in winter and summer. While the year-to-year albedo difference in west China is small.

In summer, vegetation may contribute to changes of physical features and the growing environments, such as chlorophyll, soil moisture and ground temperature, which result in more albedo change, while in the non-vegetation area, such as in snow-covered mountain areas, the summer temperature triggers snow melting, contributing to large albedo change. In winter, the albedo change in North China results from the snowfall, while the albedo change in South China results from the rainfall, evergreen trees.

3. 1.3 Albedo differences between day 353 and 321 and day 225 and 193 of 2001

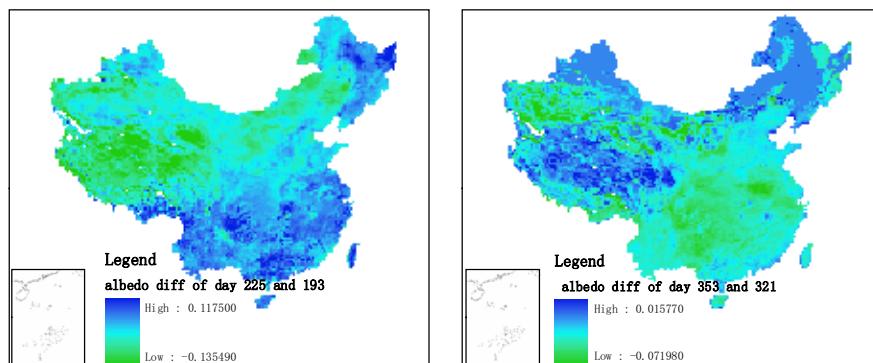


Figure 3 albedo difference chart between day 353 and 321 and between day 225 and 193 of 2001

Seen from the albedo difference chart between day 225 and 193, there appears a bias of -0.135 in the area of the Tibet Plateau, Tianshan mountain region of Xinjiang and Inner Mongolia. The largest bias in the areas of north-eastern and southern China is 0.117. From the albedo difference chart between day 353 and 321, the albedo difference is below a magnitude of 0.1, with a bias of only -0.07 in the center area of southern China, in the southern area of Xinjiang and in the north-eastern area of Tibet Plateau.

The inter-monthly albedo difference in winter can be negligible, while the inter-monthly albedo difference in summer is not negligible, pointing to the need for the land surface model to be able to parameterize accurate albedo in order to close the land surface energy budget.

3. 2 Albedo change due to different land use and land cover

Albedo variation in different land use/land cover helps us to improve simulation skill of land surface models. For different land cover, the algorithm is formulated to utilize albedo as a function of changing climatic backgrounds. For snow, with its albedo varying greatly with environmental conditions and snow properties (wetness, grain size, snow age, etc.), the overall

direct beam and diffuse ground albedo are weighted combination of soil and snow albedo determined from the fraction of the ground covered with snow. Soil albedo varies with soil saturation and soil color. For vegetation, the direct and diffuse albedo is a weighted combination of the leaf and stem reflectance calculated from the two-stream approximation. Over water surface, the surface albedo depends on the depth of water and the zenith angle of the sun. The albedo varies greatly from one to another in these four categories of land cover.

For this purpose, maximum and minimum black- and white-sky albedo are compared to highlight daily variation of albedo in different land covers. The maximum and minimum white-sky albedo is larger than black-sky albedo, except for evergreen broadleaf forest, its black-sky albedo maximum is smaller than its white-sky albedo maximum.

Cropland/natural vegetation mosaic

The maximum and minimum of white-sky albedo is about 0.1 larger than those of black-sky. The maximum of both white-sky and black-sky albedo displays an increasing-decreasing-increasing mode during day 129-289. The steep turn occurs during day 129-145 and day 273-289. The minimum of black-sky albedo changes slightly with time, while the minimum of white-sky albedo changes from 0.11 to 0.21. The range of white-sky albedo is a little larger than the one of black-sky albedo.

Grasslands

The maximum of black-sky and white-sky albedo decreases at first, and then increases slightly. The minimum of black-sky changes slowly with time, while the minimum of white-sky increases from 0.1 to 0.2.

Snow and ice

The maximum of white-sky and black-sky albedo displays an increasing mode until day 129, and then a decreasing-increasing-decreasing-increasing mode during day 129-289, with the steep change during day 129-145 and day 273-289. The melting of snow and ice may contribute to the decreasing albedo during 129-289. The minimum of black-sky and white sky albedo increases with time.

Water

It is well known that if the sun is more than 30° above the horizon (zenith angle < 60°), the water albedo is a constant 0.06, while for low sun angles, the albedo increases to as high as about 0.45 when the sun is at the horizon.

The maximum and minimum of black-sky and white-sky albedo in water change slightly. The presence of minerals and vegetation may change the albedo of water. Further studies are needed on this subject.

Barren or sparsely vegetated surfaces

The maximum and minimum of black-sky and white-sky albedo in this land use category decreases slowly, which could be attributed to the sparse vegetation.

Evergreen needle-leaf forest

The maximum and minimum of white-sky albedo increase more steeply than the ones that of black-sky albedo. The maximum of black-sky albedo and minimum of white-sky show a slight decrease during summer, associated with weak vegetation attribution of the needle-leaf, leading to the slight decrease of albedo.

Deciduous broadleaf forest

The maxima of black-sky and white-sky albedo increase in winter and spring, while decreasing in summer, which is correlated with the deciduous broadleaf forest wilting in winter and strongly growing in summer.

Evergreen broadleaf forest

The maximum and minimum of the white-sky albedo increase slowly with time; the maximum of black-sky albedo decrease decreases in summer, with values less than that of the minimum of white-sky albedo.

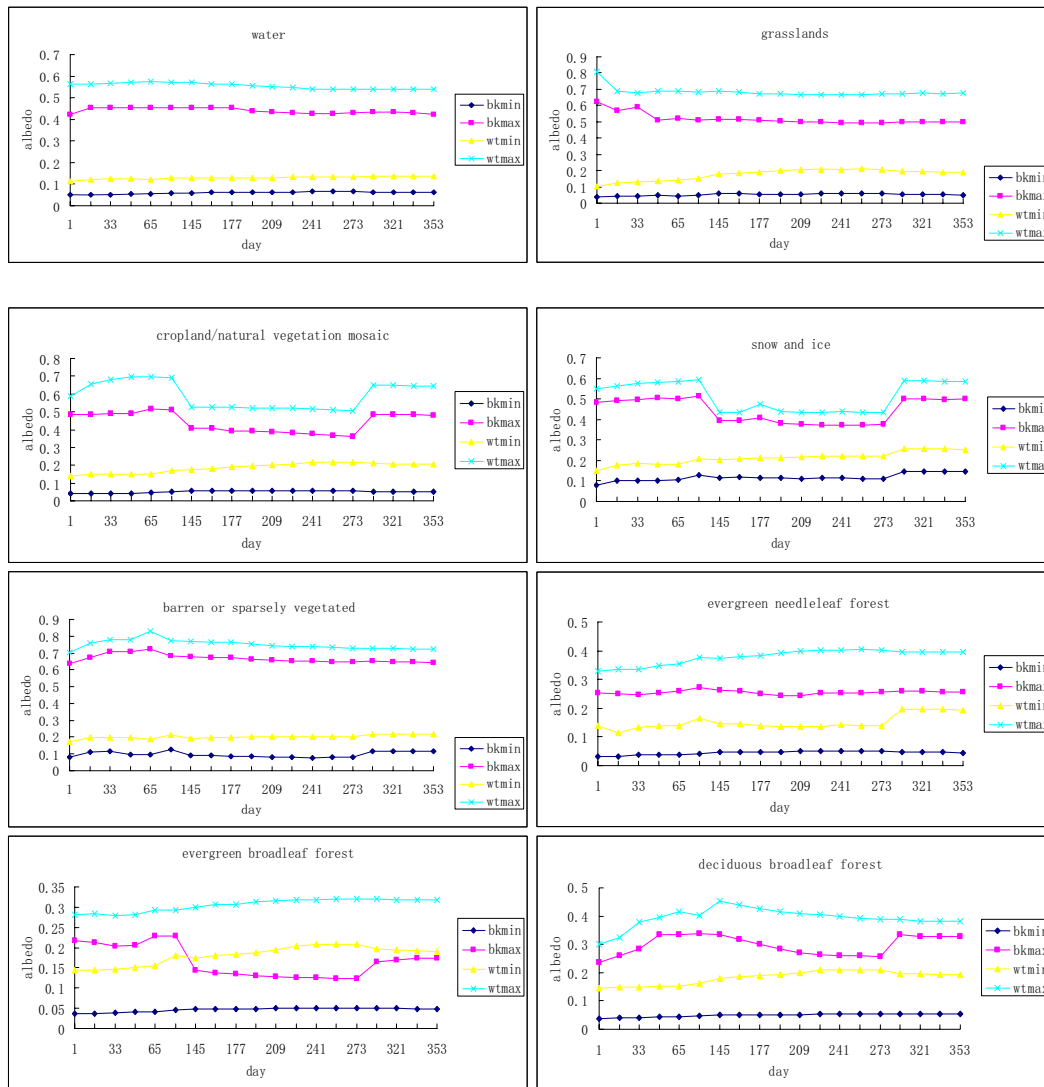


Figure 4 Albedo change due to different land use land cover with time

4.CONCLUSIONS

The inter-annual difference of albedo is large, with larger differences in east China than in west China. The 32-day difference of albedo in summer is about 0.1. The inter-annual and inter-month albedo differences are negligible. The albedo data should be introduced into land surface models to improve the albedo algorithm and data assimilation.

Black-sky albedo and white-sky albedo take on different changing features in different land cover regimes, which can serve as basic information to check physical agreement of albedo in different cover simulations.

The albedo generally decreases as one moves from grassland to evergreen needle-leaf forest to evergreen broadleaf forest and deciduous broadleaf forest; the largest intra-annual albedo variations occur over snow, cropland, evergreen broadleaf forest and deciduous broadleaf forest. Significant differences exist in albedo among broadleaved forest, needle-leaf forest, and grassland. Land cover types sharing similar albedo in winter do not necessarily share similar albedo in summer.

These results suggest that the use of overly general land cover classes (e.g., needleleaf forest, grassland) in land surface models will ignore important local-scale spatial variations in surface albedo.

ACKNOWLEDGMENTS

This work was supported by USDA UV-B Monitoring and Research Program under a grant from USDA CSREES (Agreement 2005-34263-14270), National Project for Basic Research on "Carbon Cycle and Driving Mechanisms in Chinese Terrestrial Ecosystem" (2002CB412507), National Natural Science Foundation of China (Project: 40471097), and National "973" Fundamental Pre-research Program (No. 2003ccc01500), Outstanding Overseas Chinese Scholars Fund of Chinese Academy of Sciences (2004-7-1), "Chunhui Plan" of Ministry of Education of China (Z2004-1-65010).

REFERENCE

- 1 Cess R D. Biosphere-albedo feedback and climate modeling. [J]. *Journal of the Atmospheric Sciences*. 1978, 35: 1765-1768.
- 2 Dickinson R E. Land surface processes and climate-surface albedos and energy balance. [J]. *Advance of Geophys.* 1983, 25: 305-353.
- 3 Kiehl J T, J J Hack, G B Bonan, et al., Description of the NCAR Community : Climate Model. NCAR Technical Note NCAR/TN2420 + STR, National Center for Atmospheric Research, Boulder, Colorado. 1996: 152pp.
- 4 Hu B, Lucht W, Strahler A H. The interrelationship of atmospheric correction of reflectances and surface BRDF retrieval: A sensitivity study. [J]. *IEEE Trans. Geosci. Remote Sens.*, 1999, 37: 724-738.
- 5 Vermote E F, N Z El Saleous, Justice C O. Atmospheric correction of MODIS data in the visible to middle in-fared : first results. [J]. *Remote Sensing of Environment*. 2002, 83: 97-111.
- 6 Henderson-Sellers A, Zhang Z-L, Dickinson R E. The project for intercomparison of land-surface parameterization schemes. [J]. *Bull. Am. Meteorol. Soc.*, 1993, 74: 1335-1349.
- 7 Henderson-Sellers, A., and Wilson, M. F. (1983), Surface albedo for climate modeling. *Reviews of Geophysics* 21:1743-1778.
- 8 Avissar, R., and Verstaete, M. M. (1990), The representation of continental surface processes in atmospheric models. *Reviews of Geophysics* 28:35-52.
- 9 Dickinson, R. E. (1995), Land processes in climate models. *Remote Sens. Environ.* 51:27-38.
- 10 Lofgren, B.M. Surface albedo-climate feedback simulated using two-way coupling. *Journal of Climate* 8(10):2543-2562 (1995).
- 11 Dorman J L, Sellers P J. A global climatology of albedo, roughness length and stomatal resistance for atmospheric general circulation models as represented by the Simple Biosphere model SiB. [J]. *Journal of Applied Meteorology, BRDF/Albedo*, 2005, http://modis.gsfc.nasa.gov/data/atbd/land_atbd.php. 1989, 28: 833-855.
- 12 Sellers, P. J. (1993), Remote sensing of the land surface for studies of global change, NASA/GSFC International Satellite Land Surface Climatology Project Report, Columbia, MD.
- 13 Li, Z. Q., and Garand, L. (1994), Estimation of surface albedo from space—a parameterization for global application. *J. Geophys. Res.* 99:8335-8350.
- 14 Lewis, P., Disney, M. I., Barnsley, M. J., and Muller, J.-P. (1999), Deriving albedo for HAPEX-Sahel from ASAS data using kernel-driven BRDF models. *Hydrology and Earth System Sciences* 3:1-13.
- 15 Liang S. Narrowband to broadband conversions of land surface albedo : I Algorithms [J]. *Remote Sensing of Environment* 2001, 76: 213-238.
- 16 Schaaf, C. B., et al., First operational BRDF, albedo, and nadir reflectance products from MODIS, *Remote Sens. Environ.*, 83, 135-148, 2002.
- 17 Lucht, W., Schaaf, C. B., and Strahler, A. H. (2000), An algorithm for the retrieval of albedo from space using semiempirical BRDF models. *IEEE Transact. Geosci. Remote Sens.* 38:977-998.
- 18 Martonchik, J. V., Bruegge, C. J., & Strahler, A. H. (2001). A review of reflectance nomenclature used in Remote Sensing. *Remote Sensing Reviews*, 19, 9-20.
- 19 Lucht, W., Expected retrieval accuracies of bidirectional reflectance and albedo from EOS-MODIS and MISR angular sampling, *J. Geophys. Res.*, 103, 8763-8778, 1998.
- 20 Lucht, W., and P. Lewis. Theoretical noise sensitivity of BRDF and albedo retrieval from the EOS-MODIS and MISR sensors with respect to angular sampling, *Int. J. Remote Sensing*, 21, 81-98, 2000.
- 21 Disney M, Lewis P. An investigation of how linear BRDF models deal with the complex scattering processes encountered in a real canopy. In *Proc. Int. Geosci. Remote Sens. Symp.* 98. 1998.
- 22 Hu B, W Lucht, X Li, et al., Validation of kernel-driven models for global modeling of bidirectional reflectance. [J]. *Remote Sens. Environ.*, 1997, 62: 201-214.
- 23 Roujean, M Leroy, Deschamps P Y. A bidirectional reflectance model of the Earth's surface for the correction of remote sensing data. [J]. *J. Geophys. Res.*, 1992, 97: 20455-20468.